International Journal of Engineering

Journal Homepage: www.ije.ir

Physical and Magnetic Properties Comparison of Cobalt Ferrite Nanopowder Using Sol-gel and Sonochemical Methods

P. Puspitasari*[a,b], L. S. Budi[a]

[a] *Department of Mechanical Engineering, Faculty of Engineering, State University of Malang, Indonesia*
[b] *Centre of Advanced Materials for Renewable Energy, State University of Malang, Indonesia*

PAPER INFO

Paper history:
Received 18 February 2020
Received in revised form 20 March 2020
Accepted 10 April 2020

Keywords:
Phase Identification
Morphology
Hysteresis Curve
Hyperthermia

ABSTRACT

Cobalt ferrite or $CoFe_2O_4$ has unique physical and magnetic properties depend on its synthesis method. The application of cobalt ferrite as nanomedicine material become more interesting, however analysis on physical and magnetic properties based on synthesis method have not been discussed. The cobalt ferrite in this research was synthesised using two different methods: the sol-gel with duration sintering variations of 500°C, 800°C, and 1100°C and unsintered sonochemical. The phase identification analysis and crystal size used XRD and morphology analysis used SEM, the functional group bond analysis used FTIR, and magnetic property analysis used VSM. The smallest crystal size from the XRD result was 13.25 nm with 57.04% crystallinity. The morphology from the synthesized cobalt ferrite was mostly agglomerated. The FTIR showed functional group vibration at 601-636 cm^{-1} that signified the spinel structure of the cobalt ferrite. There was a change of hysteresis loop curve from hard magnetic to soft magnetic, and there was a sample with a paramagnetic curve.

***doi**: 10.5829/ije.2020.33.05b.20*

NOMENCLATURE

D	Crystalline diameter (nm)	A	XRD diagram sample area
k	Corrective Constants (0.9)	R	Remanence Ratio
λ	Wavelength (1.5406 Å)	M_r	Magnetic Remanence (emu/g)
$FWHM$	Full-width half maximum (the peak value in radians)	M_s	Magnetic Saturation (emu/g)
θ	Peak angle (degree)	H_C	Coercivity (Oersted)
I_t	Crystalline peak intensity	K_1	Constant Anisotropy (erg/g)
I_a	Amorphous area intensity	μ_0	Permeability of Free Space (H/m)
A_{cr}	Area of crystalline XRD diagram	SLP	Specific Loss Power (W/g)
CI	Crystallinity Index		

1. INTRODUCTION

In the recent years, the fast development of nanomaterial and its application depends on synthesis methods for desired properties than the base material at nanoscale compared to macro scale [1]. Industry always needs a cheap but high-quality material, and thus, research continues and progresses to produce advanced material or nanomaterial. The example is nanomaterial synthesis from the metal-oxide type that quickly develops due to its significant ability in its application [2].

Nowadays, researchers pay attention to nanomaterial ferrite because of its wide application such as in biotechnology, for catalyst, ferrofluid, and magnetic material [3]. Ferrite, as an excellent magnetic material, attracts scientists and is continuously developed. Apart from ferrite, cobalt also has some particular property as magnetic material, for example, medium magnetization saturation, strong anisotropy, high coercivity value at room temperature, stable chemical property and high curie temperature [2]. Hence, when combined into cobalt ferrite ($CoFe_2O_4$), it has a unique magnetic property and

*Corresponding Author Institutional Email: *poppy@um.ac.id* (P. Puspitasari)

Please cite this article as: P. Puspitasari, L. S. Budi, Physical and Magnetic Properties Comparison of Cobalt Ferrite Nanopowder Using Sol-gel and Sonochemical Methods, International Journal of Engineering (IJE), IJE TRANSACTIONS B: Applications Vol. 33, No. 5, (May 2020) 877-884

is applied as supercapacitor and anode in Li-ion battery [4]. Cobalt Ferrite can also be used in medical applications because of the magnetic properties. Hyperthermia is one of a modality cancer treatments at elevated temperature between 41 ℃ and 45 ℃ and treatment time of at least 30 minutes has been paid considerable attention due to its clinical efficacies, such as minimizing clinical side effects and can selectively destroy a localized or a deeply seated cancer tumor by heating with magnetic field [5]. Well-dispersed cobalt nanoparticles in the hyperthermia application give effective and controlled heat generation [6].

Cobalt ferrite ($CoFe_2O_4$) has unique physical and mechanical properties and widely applicated in nanomedicine [6], supercapacitor and anode in Li-ion battery [4]. Cobalt ferrite is a hard magnetic material with high Curie temperature (520℃), high coercivity of around 4.3 kOe at room temperature for single domain with the size of 40 nm, medium saturation magnetization of 80 emu/g for bulk material at room temperature, high anisotropy constant ($2.65 \times 10^6 - 5.1 \times 10^6$ erg cm^{-3}) and high magnetostrictive (-225×10^{-6}). Besides, cobalt ferrite shows excellent chemical stability, mechanical hardness, wear resistance, easy to synthesis, and electrical isolation. The above properties make cobalt ferrite as one of the promising candidates in various applications.

The magnetic property of $CoFe_2O_4$ depends on the grain size and cation distribution in the form of tetrahedral and octahedral lattice [7]. Several synthesis methods to produce $CoFe_2O_4$ nanomaterial in a right nanometric scale are sol-gel and sonochemical [2, 8,9]. To date the researcher still find the best synthesis methods to obtain single phase $CoFe_2O_4$ resulted in the best magnetic properties. This research surprisingly describe how $CoFe_2O_4$ magnetic properties changing from hard magnetic to soft magnetic material as the sintering temperatures varied and also study the comparison of two synthesis methods which are sol-gel and sonochemical in term of physical and magnetic properties.

2. MATERIALS AND METHODS

2. 1. Material Preparation Raw material for cobalt ferrite is Cobalt(II) nitrate hexahydrate ($Co(NO_3)\cdot 6H_2O$ with 99% purity, Iron(III) nitrate nonahydrate ($Fe(NO_3)\cdot 9H_2O$ with 99% purity that were purchased from Merck and ethylene glycol supplied from Merck.

2. 2. The Sol-gel Method The base material in this research was 1.4505 g Cobalt(II) nitrate hexahydrate ($Co(NO_3)\cdot 6H_2O$ with 99% purity, 4.4 g Iron(III) nitrate nonahydrate ($Fe(NO_3)\cdot 9H_2O$ with 99% purity that were bought from Merck and dissolved into 50 ml ethylene glycol and was stirred for 2 hours with rotation speed of 200 rpm. Then, the solution was stirred and heated at 80℃ with a rotation speed of 200 rpm until it turned to gel. Gel formation occured in about 16.5 hours. After that, the sample was dried in the microwave oven for 7 hours at 100℃. After drying process, the sample was grinded by agate mortar for 1 hour.

2. 3. The Sonochemical Method The base material in this research were 2.951 g Cobalt(II) nitrate hexahydrate ($Co(NO_3)\cdot 6H_2O$ with 99% purity, 8.08 g Iron(III) nitrate nonahydrate ($Fe(NO_3)\cdot 9H_2O$ with 99% purity that were bought from Merck and dissolved into 100 ml DI Water. The mixture was stirred for 1 hours with rotation speed of 200 rpm. Then, the solution was stirred and heated at 80℃ with the rotation speed of 200 rpm until it turned to gel. After, the sample was sonicated for 30 minutes and titrated with 100 ml sodium hydroxide 10 M, washed with 750 ml distilled water for three times and dried in the microwave oven at 100℃. The sample was then grinding by agate mortar for 1 hour.

2. 4. Characterization The powder from the sol-gel and sonochemical synthesis methods each had yellowish-brown and darkish black colour. The cobalt ferrite from two methods then characterized to find the phase identification and crystallite size using the X-Ray Diffractometer (XRD) PAN Analytical Cu Kα (λ = 1.54 Å), morphology of $CoFe_2O_4$ obtained from Scanning Electron Microscopy of Phenom, the functional group was observed using Fourrier Transform Infrared (Shimadzu) and the magnetic properties were obtained from Vibrating Sample Magnetometer of OXFORD 1.2H at room temperature.

3. RESULTS AND DISCUSSION

3. 1. Phase Characterization The polycrystalline material properties depend on the crystal size and this fact

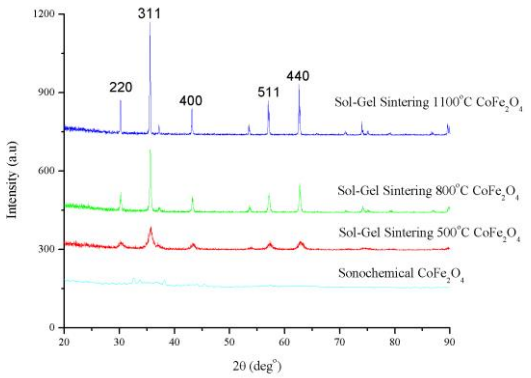

Figure 1. Phase Identification of $CoFe_2O_4$ with Different Sintering Temperature and Methods

TABLE 1. Intensity, FWHM, d-spacing, Crystallite Size of $CoFe_2O_4$ and Cristalinity

Sample Material	X-Ray Diffraction Corresponding to [311] peak				Crystallinity (%)
	Intensity (counts)	FWHM (rad)	d-spacing (Å)	Crystallite Size (nm)	
$CoFe_2O_4$ Sonochemical	24.74	0.0034	2.35897	42.71	44.17
$CoFe_2O_4$ Sol-Gel Sintering 500℃	69.05	0.0101	2.51587	13.25	57.04
$CoFe_2O_4$ Sol-Gel Sintering 800℃	226.88	0.0024	2.52141	60.5	57.67
$CoFe_2O_4$ Sol-Gel Sintering 1100℃	428.55	0.0021	2.52602	70.64	57.71

triggered several decades of research to find the nanomaterial with the best crystal size. Therefore, it is essential to measure the crystallite size of the polycrystalline material accurately. The crystallite size was calculated using the Scherrer equation [10,11].

$$D = \frac{k \times \lambda}{FWHM \times \cos\theta} \quad (1)$$

Crystallinity percentage in the samples were taken into consideration because crystallinity influences the phase and physical property. Crystalinity percentage or Segal CI (Crystallinity Index) was found by Segal et al. [12] and formulated as peak crystalline area divided by the amorph area as shown below [13]:

$$CI = \frac{It - Ia}{It} \times 100\% \quad (2)$$

Or,

$$CI = \frac{Acr}{A} \times 100\% \quad (3)$$

Figure 1 shows the significant crystallinity difference between both methods. As-sintered $CoFe_2O_4$ displays better crystallinity chart whereas the unsintered sample has lower crystallinity. Unsintered $CoFe_2O_4$ crystallinity percentage was 44.17% while the sintered samples had around 57% crystallinity. Although the sintered samples had different temperatures, but the percentage did not significantly change since at 500℃ temperature. Figure 2 presents the calculation using Equation 3 above and calculated using OriginPro software. There are peaks on Figure 1: 220, 311, 400, and 511, that were the phase identity of $CoFe_2O_4$ [14]. The same peak of 311 from sintered samples showed that the crystallinity was single phase [12].

Table 1 shows the crystal size and crystallinity index of $CoFe_2O_4$ that were synthesized using unsintered sonochemical and sintering sol-gel for 2 hours and holding temperature variations (500℃, 800℃, and 1100℃). The smallest crystal size was found in the $CoFe_2O_4$ sample sintered at 500℃ with the value of 13.25 nm. The most significant crystallinity percentage was found in the $CoFe_2O_4$ sample sintered at 1100℃, with a value of 57.71%.

Based on Figures 3(a) and (b), an increase in the temperature of sintering causing grown to the crystallite size material until 70.64 nm at sintering temperature 1100, but it did not happen with the crystallinity in the range of 500 to 1100℃ sample. The crystallinity of the sample was saturated for 57% from 500℃ until 1100℃ but increasing the crystallinity unsintered sample which was 44.17% crystallinity to 57.04%.

3. 2. Morphological Characterization The observation and comparison of morphology form were conducted using SEM. This analysis aimed to find the morphological change of $CoFe_2O_4$ from different synthesis method and different sintering temperature.

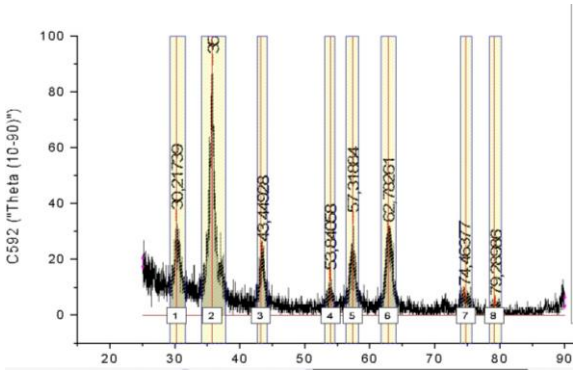

Figure 2. Crystallinity Area Measurement of $CoFe_2O_4$ with 500℃ Sintering Temperature

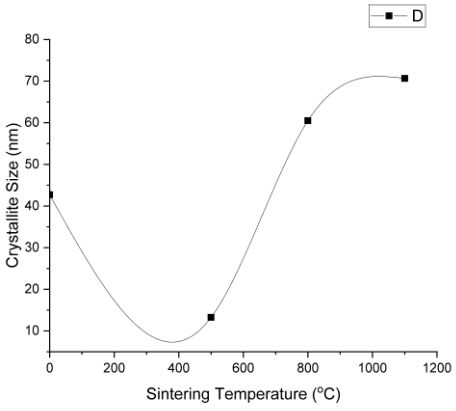

(a)

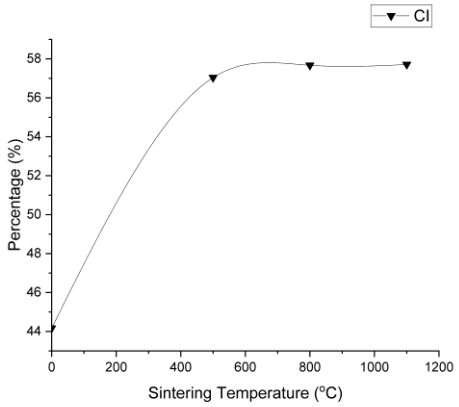

(b)

Figure 3. Comparison Effect of Sintering $CoFe_2O_4$ Samples, (a) Sintering Temperature and Crsytallite Size, (b) Sintering Temperature and Crystallinity

Figure 4(a) displays that unsintered sonochemical $CoFe_2O_4$ has morphological magnification of 25k. The grains are not homogenous but agglomerated and covered by cylindrical shape that extends into taper in various sizes, from the smallest of 34.63 nm up to the largest of 42.48 nm. Figure 4(b) presents the sintered $CoFe_2O_4$ at 500°C with 10k magnification, and the easiest spotted grain sizes are 65.94 nm up to 74.92 nm. Meanwhile, Figure 4(c) shows the sintered $CoFe_2O_4$ at 800°C with 10k magnification. The observed grains are between 59.79 nm until 73.72 nm. Figure 4d displays the sintered $CoFe_2O_4$ at 1100°C with 10k magnification. The grain sizes start from 50.98 nm up to 56.98 nm.

The SEM image analysis present that agglomeration in all samples was still high as observed the decreasing agglomeration from the sintering at 500°–1100°C due to the crystalline development in the sintering process [15].

The crystalline growth caused the grain size in SEM morphology to be small. The sintered $CoFe_2O_4$ at 500°C had crystal size of 13.25 nm and SEM results around 70 nm, the crystal size continued to grow up to 70.64 nm with the grain size from SEM results was 52 nm for sintered $CoFe_2O_4$ at 1100°C. The sonochemical $CoFe_2O_4$ had a crystal size of 42.71 nm, and the SEM grain results were around 27 nm. However, it had the lowest crystallinity percentage than the other three samples with a value of 44.17%. Sintering causes crystal size to grow and lower the agglomeration, as shown in Figure 4d where the agglomeration was reduced compared to other samples. High agglomeration was a possibility caused by Van der Waals forces that weaken the bonds between particle [16]. In general, the SEM grain was spherical, but some was elongated.

3. 3. FTIR Analysis The FTIR spectrum was used to identify the chemical compound structure and found the spinel phase formation of the synthesized $CoFe_2O_4$ [16].

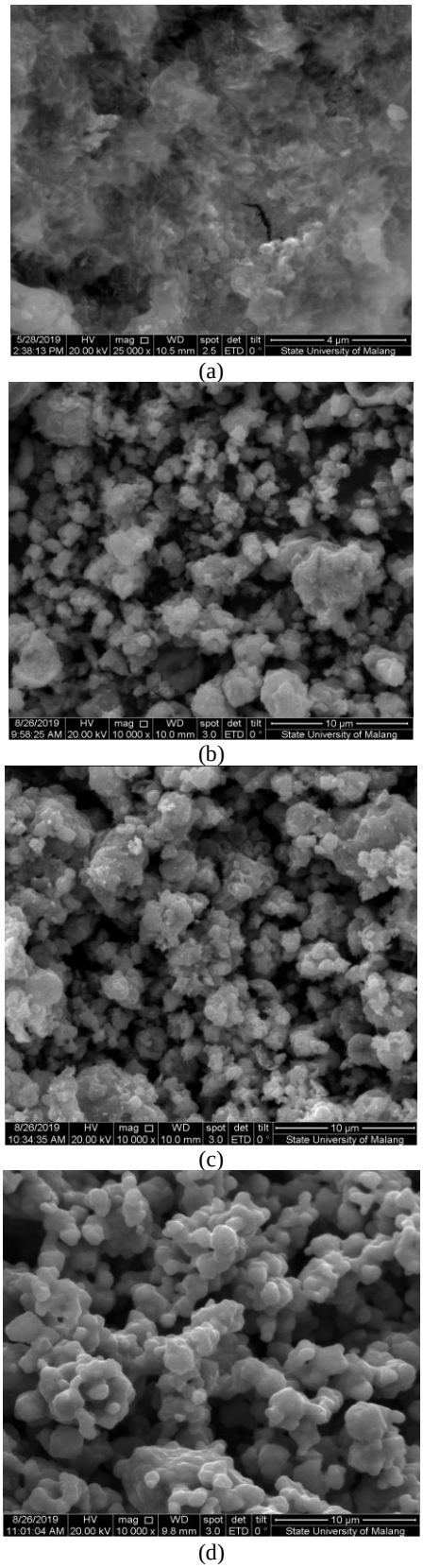

(a)

(b)

(c)

(d)

Figure 4. Morphology of $CoFe_2O_4$, (a) Sonocehmical without Sintering, (b) Sol-gel 500°C Sintering, (c) Sol-gel 800°C Sintering, (d) Sol-gel 1100°C Sintering

Figure 5 shows the comparison of the FTIR spectrum from four samples with three main zones analysis. There are several peaks based on various treatments in the first zone, 636 cm^{-1} for sonochemical method, sol-gel 500℃ sintering 601 cm^{-1}, sol-gel 800℃ sintering 619 $cm^{-1}$and sol-gel 1100℃ sintering 623 cm^{-1}.The first zone was indicated the area stretching vibration from the metal-oxygen (M–O, where M = Co or Fe) that showed identity and finger print zone from the $CoFe_2O_4$ absorption band [17].

The difference in the absorption position in the first zone that was the fingerprint of $CoFe_2O_4$ due to the crystal size are variated. The variated crystal size will make difference distance between Fe^{3+}-O^{2-} then the absorption will slightly difference between the samples. The second zone compound several peaks based on the samples, there are 1456 cm^{-1} for sonochemical method, sol-gel 500℃ sintering 1531 cm^{-1}, sol-gel 800℃ sintering 1427 cm^{-1}, sol-gel 1100℃ sintering 1409 cm^{-1}.

The second zone indicated bending vibration and stretching vibration from the hydroxyl (-OH) functional group as one of the characteristics of water absorption bands [18] the adsorbed water is featured by the bands at 1409-1531 cm^{-1}assigned to the δ H-O-H bonding mode [19]. From the second zone, we can imply that water molecules does not get totally remove from the sample although there are several heat treatments applied to the samples.

The third zone had several differences, but for the sonochemical $CoFe_2O_4$, peak 3423 cm^{-1} and 3412 cm^{-1} could not be observed as well as the spectrum of the sintered sample at 1100℃. The both peaks have been assigned to antisymmetric and symmetric O-H stretching vibration of lattice water. Thus, this situation followed the sintering process that omits water content because the sample was sintered at 1100℃.

Meanwhile the sonochemical sample lost the peak due to the long duration of drying. The second zone peak's appeared on all synthesised samples because this is the water molecule identity. This peak experienced intensity decrease along with the increasing sintering temperature that proved the sintering temperature reduces water molecule as well as water absorption by other molecules and thus make the intensity to decrease [19]. Also different methods proved that sol-gel samples had higher water content as seen from the peak intensity of the second zone and the third zone because the synthesis process form sol then followed by liquid compaction into a gel that will not be separated easily from the content of water molecules in it.

$$R = \frac{Mr}{Ms} \quad (4)$$

3. 4. Magnetic Properties Analysis The magnetic property of $CoFe_2O_4$ that was synthesized was obtained from the VSM test such as magnetic saturation (M_s), magnetic remanence (M_r), and coercivity (H_c) [20]. M_s is the maximum value of magnetization that is received from the given magnetic field. The value of M_r can be taken from the intersection of curves that intersect with the vertical axis. H_c is the magnetic field intensity needed to make the magnetic sample reach zero magnetization after achieving magnetization saturation. Remanence ratio is the ability of magnetic material to change the curve in the hysteresis loop curve after the magnetic field is removed [21]. The value of parametere above was described in Table 2. Remanence ratio can be formulated [22].

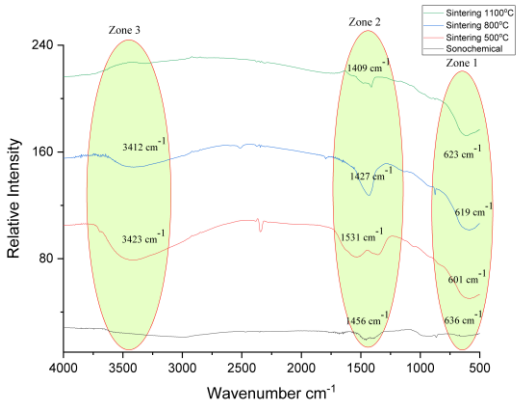

Figure 5. FTIR Spectra Analysis of $CoFe_2O_4$ with Different Sintering Temperatur and Methods

TABLE 2. Magnetic Saturation, Magnetic Remanence, Coercivity and Remanence Ratio

Sample Material	Magnetic Saturation/M_s (emu/g)	Magnetic Remanence/M_r (emu/g)	Remanence Ratio/ R	Coercivity/H_C	
				T	Oe
$CoFe_2O_4$ Sonochemical	1.29	0.06	0.046	0.0012	12
$CoFe_2O_4$ Sol-Gel Sintering 500℃	89.02	41.83	0.469	0.1032	1032
$CoFe_2O_4$ Sol-Gel Sintering 800℃	113.51	23.4	0.206	0.472	472
$CoFe_2O_4$ Sol-Gel Sintering 1100℃	4.18	0.17	0.040	0.0066	66

Figure 6 shows the comparison of the hysteresis loop curve from the synthesized $CoFe_2O_4$. The hysteresis loop curve of the sintered sample at 500℃ indicated hard magnetic material, sintered sample at 800℃ indicated soft magnetic material, while the sintered sample at 1100℃ and sonochemical sample indicated paramagnetic material [23]. The change from hard magnetic into soft magnetic occurred in 500℃ to 800℃ sintering temperature. Changes in the curve are thought to be due to the sintering temperature which has exceeded its temperature (520℃) [7] thereby reducing M_r and H_C; the change was due to the transition from a single domain to multi-domain [14]. The transition change was caused by the critical diameter of $CoFe_2O_4$ that was 40 nm according to Figure 7, and thus, after passing the critical diameter, the coercivity was reduced [24, 25].

With the decrease of H_c, there was an increase of M_s from 89.02 emu/g to 113.5 emu/g following the Brown's equation as follows [14, 27]:

$$Hc = \frac{2K1}{\mu 0 Ms} \quad (5)$$

An increase in sintering temperature from 500℃ to 800℃ made the H_c value changed from 1032 Oe to 472 Oe and thus narrow down the curve. This phenomenon made the grain size uneven and agglomerated, as shown in Figure 4 where agglomeration decreases following the decreasing H_c. An increase in sintering temperature around 500℃ to 800℃ caused the crystal grain to grown from 13.25 nm to 60.5 nm, and the H_c value decreased [23]. Sintered $CoFe_2O_4$ at 1100℃ had paramagnetic curve caused by the sintering temperature that passed the Curie temperature and made the magnetic property to dissolve, whereas the sonochemical sample was thought to have paramagnetic curve because the NaOH titration that has not entirely disappeared in the sample. All samples had remanence ratio below 0.5, thus if R <0.5, there was a static magneto interaction between the granules [27].

Figure 8 explains the relationship between crystal size with M_s and H_c. Comparison of crystallite size to M_s shows that there is the largest M_s value in crystallite size of 60.5 nm and 113.51 emu/g. The 13.25 nm crystal size has a M_s value of 89.02 but has the greatest coercivity value of all samples, which is 1032 Oe. This phenomenon occurs because the crystal size has a magnetic domain in the form of a single domain, this phenomenon has been explained in the explanation above. From Figure 8 we can say that after critical diameter the magnetic curve of M_s and H_c will be downward curve due the transiton from single domain to multi domain magnetic. From the results above we can also conclude that cobalt ferrite sol-gel with sinterring 500℃ have a high magnetic saturation and high coercivity also smaller crystallite size that can be applied to Hyperthermia.

In the application of hyperthermia, it requires several important parameters, such as high $M_{s\ and}$ H_c values so that it can quickly kill cancer cells but dissolved particles must be small in size. Based on reported data by Yadavalli et al. [28] nanomaterials $CoFe_2O_4$ with crystallite size 19.8 nm have M_s and H_c about 59 emu/g and ± 300 Oe, which was the best results for their experiment to hyperthermia study. Darwish et al. [29] reported nanomaterials $CoFe_2O_4$ with crystallite size 32.46 nm have M_s about 50.61 emu/g with applicate to hyperthermia have *SLP* value about 552 W/g. Rashad et al. [30] reported nanomaterials $CoFe_2O_4$ with crystallite size 10.7 nm have M_s and H_c about 36.2 emu/g and 513.2 Oe with applicate to hyperthermia have *SLP* value about 302 W/g. Nam et al. [31] reported nanomaterials $CoFe_2O_4$ with crystallite size 11 nm have M_s about 58 emu/g which is applicable to hyperthermia have *SLP* value about 297 W/g. Yasemian et al. [32] also reported nanomaterials $CoFe_2O_4$ having crystallite size 11.1 nm have M_s and H_c about 42.94 emu/g and 169.19 Oe with

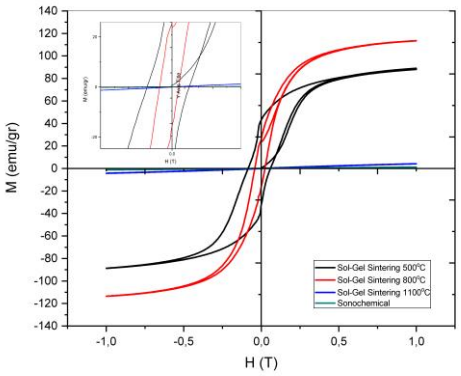

Figure 6. Magnetic Hysteresis Curve of $CoFe_2O_4$, (black) Sol-gel 500℃ Sintering, (red) Sol-gel 800℃ Sintering, (blue) Sol-gel 1100℃ Sintering, (light green) Sonochemical without Sintering

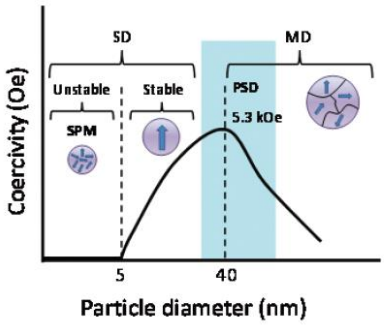

Figure 7. Dependence of coercivity with particle diameter for cobalt ferrite [25].

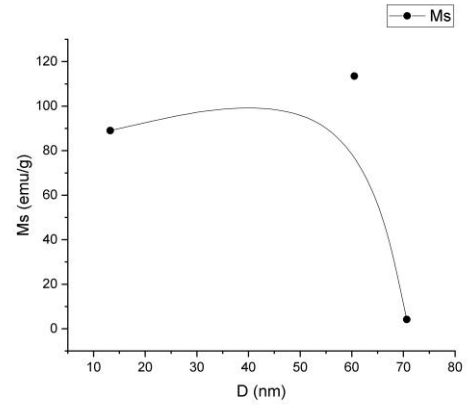

(a)

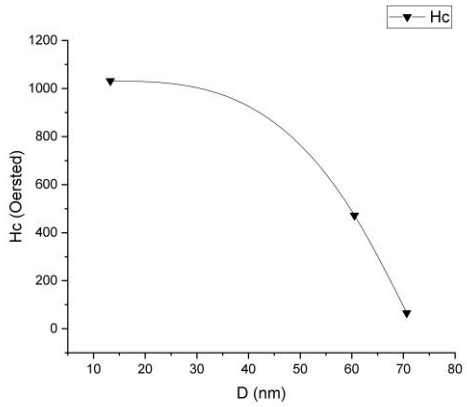

(b)

Figure 8. Comparison of Sol-Gel $CoFe_2O_4$ Samples, (a) Crsytallite size and Magnetic Saturation, (b) Crsytallite size and Coercivity

applicate to hyperthermia have *SLP* value about 395 W/g. Based on the research mentioned above, the cobalt ferrite sol-gel with sintering 500℃ with crystallite size 13.25 nm have a big potential to applicate to hyperthermia due the M_s and H_c greater than mentioned before also will be easily dispersed.

4. CONCLUSION

The synthesized cobalt ferrite with two methods, unsintered sonochemical and sintered sol-gel at 500℃, 800℃, and 1100℃ for 2 hours had cubic spinel structure with the smallest crystal size of 13.25 nm and the largest of 70.64 nm following the increasing sintering time, the lowest crystallinity of 44.16% and the highest of 57.7%. The SEM results showed that the morphology of cobalt ferrite was decreasing agglomeration and smaller grain size following the high sintering temperature. The FTIR analysis presented functional group vibration at 601-636 cm^{-1} that signified the spinel structure identity. The VSM results showed a change in hysteresis loop curve from the sintered samples at 500℃ and 800℃ from hard magnetic into soft magnetic material. The curve difference was due to the high temperature that passed the Curie temperature and due to the transition from the single domain into multiple domains as shown by the Brown equation. The SEM results displayed the decreasing agglomeration because of the sintering temperature that passed the Curie temperature and decreased the magnetic property. Based on research that already mentioned, cobalt ferrite sol-gel sintering 500℃ had big potential to applicate on hyperthermia.

5. REFERENCES

1. Yadav RS, Kuřitka I, Vilcakova J, Havlica J, Kalina L, Urbánek P, Machovsky M, Skoda D, Masař M, Holek M (2018) Sonochemical synthesis of Gd3+ doped $CoFe_2O_4$ spinel ferrite nanoparticles and its physical properties. Ultrason Sonochem, Vol. 40, 773-783
2. Karthigayan N, Manimuthu P, Priya M, Sagadevan S (2017) Synthesis and characterization of $NiFe_2O_4$, $CoFe_2O_4$ and CuFe2O4 thin films for anode material in Li-ion batteries. ***Nanomaterials and Nanotechnology***, Vol. 7, 1-5
3. Goswami PP, Choudhury HA, Chakma S, Moholkar VS (2013) Sonochemical synthesis of cobalt ferrite nanoparticles. ***International Journal of Chemical Engineering***. https://doi.org/10.1155/2013/934234
4. Jun G, Liping J, Junjie Z "Crystal formation and growth mechanism of inorganic nanomaterials in sonochemical syntheses", ***Science China Chemistry,*** Vol. 55, (2012), 2292-2310.
5. Mazario E, Menéndez N, Herrasti P, Cañete M, Connord V, Carrey J, "Magnetic hyperthermia properties of electrosynthesized cobalt ferrite nanoparticles", ***The Journal of Physical Chemistry C***, Vol. 117, (2013), 11405-11411
6. Amiri S, Shokrollahi H "The role of cobalt ferrite magnetic nanoparticles in medical science", ***Materials Science Engineering C***, Vol. 33, (2013), 1-8.
7. Zheng JC, Shen XQ, Min CY, Meng XF, Liang QR, "Fabrication and characterization of heterostructural $CoFe_2O_4$/ $Pb(Zr0.52Ti0.48)O_3$ nanofibers by electrospinning", ***Journal of Composite Material,*** Vol. 44, (2010), 2135-2144
8. Ismail W.N.W., Sol–gel technology for innovative fabric finishing-A Review. ***Journal of Sol-Gel Science and Technology,*** Vol. 78 No. 3, (2016), 698-707.
9. Rajan Babu D, Venkatesan K, "Synthesis of nanophasic $CoFe_2O_4$ powder by self-igniting solution combustion method using mix up fuels", ***Journal of Crystal Growth,*** Vol. 468, (2017), 179-184
10. Muniz FTL, Miranda MAR, Morilla Dos Santos C, Sasaki JM "The Scherrer equation and the dynamical theory of X-ray diffraction", Acta Crystallography Section A, Vol. 72, (2016), 385-390.
11. Sasongko MIN, Puspitasari P, Yazirin C, Tsamroh DI, Risdanareni P, "Morphology and phase identification of micron to nanosized manganese oxide (MnO) with variations in sintering time", AIP Conference Proceedings. (2017), https://doi.org/10.1063/1.5003520
12. Nam S, French AD, Condon BD, Concha M, "Segal crystallinity index revisited by the simulation of X-ray diffraction patterns of cotton cellulose Iβ and cellulose II", ***Carbohydrate Polymers,*** Vol. 135, (2016), 1-9

13. Ahvenainen P, Kontro I, Svedström K, "Comparison of sample crystallinity determination methods by X-ray diffraction for challenging cellulose I materials", ***Cellulose***, Vol. 23, (2016), 1073-1086.
14. Xavier S, Jiji MK, Thankachan S, Mohammed EM "Effect of sintering temperature on the structural and electrical properties of cobalt ferrite nanoparticles" AIP Conference Proceedings, Vol. 1576, 98-101
15. Huixia F, Baiyi C, Deyi Z, Jianqiang Z, Lin T "Preparation and characterization of the cobalt ferrite nano-particles by reverse coprecipitation" ***Journal of Magnetism and Magnetic Materials,*** Vol**.** 356, (2014), 68-72
16. Sagadevan S, Podder J, Das I "Recent trends in materials science and applications - Nanomaterials, Crystal Growth, Thin films", Quantum Dots, & Spectroscopy (Proceedings ICRTMSA 2016). 189, (2017), 145–152
17. Mohamed RM, Rashad MM, Haraz FA, Sigmund W "Structure and magnetic properties of nanocrystalline cobalt ferrite powders synthesized using organic acid precursor method", ***Journal of Magnetism and Magnetic Materials,*** Vol. 322, (2010), 2058-2064
18. Pasupong P, Choojun K, Vittayakorn N, Seeharaj P, "Synthesis of nanocrystalline cobalt ferrite by the sonochemical method in highly basic aqueous solution" ***Key Engineeing Materials Vol***. 751 KEM, (2017), 368-373
19. Pauline S, Amaliya a P "Synthesis and Characterization of Highly Monodispersive $CoFe_2O_4$ Magnetic Nanoparticles by Hydrothermal Chemical Route", ***Archives of Applied Science Research,*** Vol. 3, (2011), 213-223
20. Sabeeh SH, Sabeeh ZSA (2017) Preparation and Studying Magnetic Properties of Cobalt Ferrite (CoFe $CoFe_2O_4$) Material. International Journal of Science Engineering Research Vol. 8, No. 3, 332514248
21. Kanagesan S, Hashim M, Tamilselvan S, Alitheen NB, Ismail I, Syazwan M, Zuikimi MMM, "Sol-gel auto-combustion synthesis of cobalt ferrite and it's cytotoxicity properties", ***Digest Journal of Nanomaterials & Biostructures*** Vol. 8, No. 4, (2013), 1601-1610.
22. Xu S, Ma Y, Geng B, Sun X, Wang M "The remanence ratio in $CoFe_2O_4$ nanoparticles with approximate single-domain sizes", Nanoscale Research Letters, Vol. 11, No. 1, (2016), 1-9.
23. David Jiles "Introduction to Magnetism and Magnetic Materials" Springer-Scffince+Business Media, B.V. (1991).
24. Afshari M, Rouhani Isfahani AR, Hasani S, Davar F, Jahanbani Ardakani K "Effect of apple cider vinegar agent on the microstructure, phase evolution, and magnetic properties of CoFe2O4 magnetic nanoparticles", ***International Journal of Applied Ceramic Technology,*** Vol. 16, No. 4, (2019), 1612-1621
25. Perales-Pérez O, Cedeño-Mattei Y (2017) Optimizing Processing Conditions to Produce Cobalt Ferrite Nanoparticles of Desired Size and Magnetic Properties. ***Magnetic Spinels-Synthesis, Properties and Applications***. https://doi.org/10.5772/66842
26. Goodarz Naseri M, Saion EB, Abbastabar Ahangar H, Shaari AH, Hashim M, "Simple synthesis and characterization of cobalt ferrite nanoparticles by a thermal treatment method" ***Journal of Nanomaterials,*** (2010). https://doi.org/10.1155/2010/907686
27. El-Okr MM, Salem MA, Salim MS, El-Okr RM, Ashoush M, Talaat HM "Synthesis of cobalt ferrite nano-particles and their magnetic characterization", ***Journal of Magnetism and Magnetic Materials,*** Vol. 323, (2011), 920-926.
28. Yadavalli T, Jain H, Chandrasekharan G, Chennakesavulu R, "Magnetic hyperthermia heating of cobalt ferrite nanoparticles prepared by low temperature ferrous sulfate based method", AIP Advances, (2016), https://doi.org/10.1063/1.4942951
29. Darwish MSA, Kim H, Lee H, Ryu C, Lee JY, Yoon J, "Synthesis of magnetic ferrite nanoparticles with high hyperthermia performance via a controlled co-precipitation method", ***Nanomaterials,*** (2019), https://doi.org/10.3390/nano9081176.
30. Rashad MM, Mahmoud SM, Abdel-Hamid Z, El-Sayed HM, Shalan AE, Khalifa NA, Kandil AT, "Structural, magnetic properties, and induction heating behavior studies of cobalt ferrite nanopowders synthesized using modified co-precipitation method", ***Particulate Science and Technology,*** Vol. 36, No. 2, (2018), 172-177
31. Nam PH, Lu LT, Linh PH, Manh DH, Thanh Tam LT, Phuc NX, Phong PT, Lee IJ, Polymer-coated cobalt ferrite nanoparticles: Synthesis, characterization, and toxicity for hyperthermia applications. ***New Journal of Chemistry***, Vol. 42, (2018), 14530-14541.
32. Yasemian AR, Almasi Kashi M, Ramazani A, "Exploring the effect of Co concentration on magnetic hyperthermia properties of $Co_xFe_{3-x}O_4$ nanoparticles" ***Materials Research Express,*** Vol. 7, (2020), 016113.

Persian Abstract

چکیده

فریت کبالت یا CoFe2O4 دارای خواص فیزیکی و مغناطیسی منحصر به فردی هستند که به روش سنتز آن بستگی دارد. استفاده از فریت کبالت به عنوان ماده نانومواد جالب تر می باشند ، اما تجزیه و تحلیل خواص فیزیکی و مغناطیسی بر اساس روش سنتز مورد بحث قرار نگرفته است. فریت کبالت در این تحقیق با استفاده از دو روش مختلف سنتز گردید: سل-ژل با مدت زمان تغییرات تغییرات پراکندگی ۵۰۰ ، ۸۰۰ و°C ۱۱۰۰ و سونوشیمیایی بدون هدف. تجزیه و تحلیل شناسایی فاز و اندازه کریستال XRD و آنالیز مورفولوژی از SEM ، آنالیز پیوند گروهی کاربردی FTIR و تجزیه و تحلیل خاصیت مغناطیسی از VSM استفاده شده است. کوچکترین اندازه بلور از نتیجه XRD 13.25 نانومتر با بلوریت ۵۷.۰۴٪ بود. مورفولوژی حاصل از فریت کبالت سنتز شده بیشتر آگلومره بود. FTIR ارتعاش گروه عملکردی را در cm^{-1} ۶۰۱-۶۳۶ نشان داد که حاکی از ساختار اسپینل فریت کبالت است. تغییری در منحنی حلقه هیسترزیس از مغناطیسی سخت به مغناطیسی نرم وجود دارد و نمونه ای با منحنی پارامغناطیسی وجود دارد.